

Accepted Manuscript

Theoretical calculation of the physico-chemical properties of 1-butyl-4-methylpyridinium based ionic liquids

Artur Giełdoń, Maciej Bobrowski, Aleksandra Bielicka-Giełdoń, Cezary Czaplewski

PII: S0167-7322(16)33119-1
DOI: doi: [10.1016/j.molliq.2016.11.087](https://doi.org/10.1016/j.molliq.2016.11.087)
Reference: MOLLIQ 6634

To appear in: *Journal of Molecular Liquids*

Received date: 17 October 2016
Accepted date: 25 November 2016

Please cite this article as: Artur Giełdoń, Maciej Bobrowski, Aleksandra Bielicka-Giełdoń, Cezary Czaplewski, Theoretical calculation of the physico-chemical properties of 1-butyl-4-methylpyridinium based ionic liquids, *Journal of Molecular Liquids* (2016), doi: [10.1016/j.molliq.2016.11.087](https://doi.org/10.1016/j.molliq.2016.11.087)

This is a PDF file of an unedited manuscript that has been accepted for publication. As a service to our customers we are providing this early version of the manuscript. The manuscript will undergo copyediting, typesetting, and review of the resulting proof before it is published in its final form. Please note that during the production process errors may be discovered which could affect the content, and all legal disclaimers that apply to the journal pertain.



Theoretical calculation of the physico-chemical properties of 1-butyl-4-methylpyridinium based ionic liquids.

Artur Gieldoń^{1,2}, Maciej Bobrowski², Aleksandra Bielicka-Gieldoń¹, Cezary Czaplewski^{1,2,*}

¹Faculty of Chemistry, University of Gdańsk, Wita Stwosza 63, 80-308 Gdańsk, Poland,

²Faculty of Technical Physics and Applied Mathematics, Technical University of Gdańsk, Naturowicza 11/12, 80-233 Gdańsk, Poland

*Corresponding author, e-mail cezary.czaplewski@ug.edu.pl

Abstract

Ionic liquids (ILs) have attracted much attention for their unique physicochemical properties, which can be designed as needed by altering the ion combinations. Besides experimental work, numerous computational studies have been concerned with prediction of physical properties of ILs. The results of molecular dynamics simulations of ILs depend strongly on the proper force field parameterization. Classical force fields and the force fields designed specifically for ILs have been found to yield diffusion coefficients, that are too low for the liquid state. This has been attributed to the lack of electronic polarizability in the most force fields. One simple solution to this problem has been uniform by scaling down of the partial charges of all ions. In this work we investigated the influence of the charge scaling, the size of the simulated system and the temperature factor on calculated density, radial distribution function and the diffusion coefficients of the cation and anion of two methylpyridinium based ionic liquids: 1-butyl-4-methylpyridinium tetrafluoroborate ([b4mpy][BF₄]) and 1-butyl-4-methylpyridinium chloride ([b4mpy][Cl]). We show that the parameterization is the key for a proper reproduction of the diffusion coefficient and as a consequence the melting temperature and ionic conductivity. We were also able to get some structural informations on the cation-anion relationships in the investigated ILs.

Keywords:

Molecular Dynamics, Ionic Liquids, 1-butyl-4-methylpyridinium, ([b4mpy][BF₄]), ([b4mpy][Cl]), charge distribution, density calculation, melting point calculation,

Introduction

Ionic liquids (IL) are novel organic salts generally composed of an organic cation and an anion, which is usually inorganic. It is known that ionic liquids exhibit extremely low vapor pressure, thermal stability up to 400 °C and relatively low flammability. The unique physicochemical properties of ionic liquids make them a good replacement of standard organic solvents in a great number of different chemical reactions. Due to the chemical stability and possibility of the recycled usage, the ionic liquids are in the field of interest of the industry [1,2]. The properties of IL can be modified by simple changes in the nature of the cation or anion. The knowledge of the way how to change physicochemical properties of ionic liquids is crucial for their optimized design [3,4]. According to Katrizky et al., there are approximately 10^{18} anion-cation combinations [5], therefore all methods which can be used for prediction of some IL properties can be extremely useful.

Theoretical chemistry offers three ways of the prediction of ionic liquid properties. Quantitative structure – property relationship (QSPR) methods are based on the extrapolation of already known or calculated properties of the training set of molecules. The newly built model of relationship can be used for a prediction of the specific properties for the new molecules [6,7,8,9]. Semi-empirical and *ab-initio* methods can be used to calculate the electron density (charge distribution, polarizability), molecular geometry and volume of the ion pairs [10,11]. The high correlation between molecular volume and basic physicochemical properties for the ionic liquids was shown by Slattery et al [12] and Wilenska et al [13]. Empirical force field and molecular dynamics methods (MD) can be used for the prediction almost all physicochemical properties of ionic liquids, however as it is shown in this study the obtained results are highly dependent on the simulation parameters.

Molecular dynamics simulations of ionic liquids are performed for almost 20 years [14,15]. Lee and co workers studied the ionic conductivity for 1-n-butyl-3-methylimidazolium ionic liquids with 1 ns molecular dynamics and show, that the self-diffusion coefficient of ionic liquids is an important factor in determination of the ionic conductivity [16]. Prado and Freitas aimed to investigate relationships between structure and thermodynamical properties of the 1-butyl-3-methylimidazolium tetrafluoroborate by using 5 ns MD simulation and OPLS-AA force field and show the difference between the diffusion of the cation and anion [17]. Kodderman and co workers calculated viscosities for imidazolium-based ionic liquids by using Green-Kubo relation and 10 ns MD and show that the parameterization of the force field is crucial in the investigation of the ILs properties [18]. Picalek and co workers investigated the surface and IL-water interface of aqueous solutions of 1-butyl-3-methylimidazolium



tetrafluoroborate with 4 ns MD and MACSIMUS package and show that the surface tension can be reproduced only by the polarizable force fields [19]. Zhang and Maginn compared several methods for calculation of the melting point temperature using molecular dynamics simulations for 1-n-butyl-3-methylimidazolium chloride [bmim][Cl] [20]. They postulate, that the pseudo-supercritical path (PSCP) method is reliable for prediction of the melting point temperature. The effects of linear scaling of the atomic point-charges were investigated by Youngs and Hardacre for the imidazolium based ionic liquid [21]. They show correlation between the charge scaling factor and the diffusion coefficient. Kowsari and co workers calculated dynamics and diffusion coefficient [22] and transport coefficients [23] of twelve 1-alkyl-3-methylimidazolium-based ionic liquids by using OPLS and AMBER forcefield. They show that the Green-Kubo relation gives lower values for electrical conductivity than the Nerst-Einstein relation. Kislenco and co workers studied the electrochemical interface between a graphite surface and the 1-butyl-3-methylimidazolium with 4 ns MD and AMBER forcefield [24]. They observed, confirmed experimentally, formation of the interfacial layers. It has been demonstrated, that enzymes are stabilized in several ILs well beyond room temperature. Klahn and co workers investigated the stability of the lipase enzyme in several ionic liquids by using GROMACS package [25].

Herein, we report the results of our theoretical studies on two ILs: 1-butyl-4-methylpyridinium tetrafluoroborate ([b4mpy][BF₄]) (CAS Number 343952-33-0) and 1-butyl-4-methylpyridinium chloride ([b4mpy][Cl]) (CAS Number 112400-86-9) by molecular dynamics (MD) simulation. The most available literature data on ([b4mpy][BF₄]) describes viscosity [26,27,28,29,30,31,32] and density [28,29,31,32,33] as measured in a function of the temperature. There are also a substantial amount of literature data according physicochemical properties of binary [26,34,35,36,37] and ternary [38] systems of ([b4mpy][BF₄]). It is known, that ([b4mpy][BF₄]) improves enantioselectivity of lipases [39], can be used as a solvent for separation of n-alkanes [40,41] and has an inhibition effect of the copper corrosion [42]. There is also information on ([b4mpy][BF₄]) toxicity [2,43,44]. The melting temperature of ([b4mpy][BF₄]) is 303 K [45]. If we compare it with 301 K of ([b2mpy][BF₄]) [46] we can conclude, that isomerization of the 1-butyl-4-methylpyridinium cation seems to have a slight effect on the melting temperature.

With our best knowledge there is only one theoretical work on ([b4mpy][BF₄]) [47]. The authors used COSMO-RS method to reproduce the excess enthalpy and solubility of the binary mixtures containing ([bXmpy][BF₄]) and B₂(CH₂)_vBr (X=2-4; v=2-6). The anion BF₄⁻ can be considered as a hydrogen bond acceptor and the hydrogen atoms of the pyridine ring



can act as donors. The alkyl group of the cation promotes interactions with apolar compounds [47]. [b4mpy][Cl] can exist in two forms, the first is solid with a melting temperature of about 332 – 334 K, the second comes from the crystallization from dry acetone and form of a white highly hygroscopic needles with the melting temperature ranges between 430 and 433K [48]. If we compare the melting temperature of the first polymorphic form with 368 K [49], 384 K [50] and 370 K [51] of [b3mpy][Cl]) we can make the same conclusion as in the case of ([b4mpy][BF₄]) that isomerization of the 1-butyl-4-methylpyridinium seems to have a small effect on the melting temperature. Ellis and coworkers investigated the usage of ([b4mpy][Cl]) with AlCl₃ as a solvent for the linear dimerisation of but-1-ene in biphasic mode [52].

In this work we investigated the influence of the charge distribution, the size of the simulated system and the temperature factor on calculated density, radial distribution function and the mobility of the cation and anion. Additionally we investigated the influence of the anion and verified, if the molecular dynamics is able to predict the state of the simulated chemical specimen (liquid or solid at given temperature).

Methods

1-butyl-4-methylpyridinium tetrafluoroborate ([b4mpy][BF₄]) and 1-butyl-4-methylpyridinium chloride ([b4mpy][Cl]) were parameterized by using the antechamber program from AMBER v.12 [53,54] package. The partial charges of cation and anion were fitted to ± 1 (Fig 1.). Three different molecular systems for both ionic liquids were built by placing 6x6x6, 8x8x8 and 10x10x10 unit boxes in the x, y and z dimensions and with a volume of each unit box of about 2000 Å³. We assume that every pair of cation and anion can occupy one unit box. In the next step we performed 2 ns molecular dynamics simulation with a temperature set to 300 K and NTP ensemble. The initial density of each simulated molecular system was about 0.2 g/cm³ and the equilibrium density was reached after 1 ns in all simulations. This procedure let us to obtain the quasi random IL structure which was used for a further investigation. Following, in all of the newly obtained IL molecular systems (three of ([b4mpy][BF₄]) and three of ([b4mpy][Cl]) with a size of 6³, 8³ and 10³ cation - anion pairs), the partial charges were scaled by a factor of 1.0, 0.96, 0.92 and 0.88 and simulated in time of 10 ns in five different temperatures: 270, 300, 330, 360 and 390 K by using MD as implemented in AMBER v.12 package [53]. The General AMBER force field (GAFF) was already used with a success for prediction of some thermodynamic properties of the ionic liquids [24,55,56]. All simulations were done with the following conditions: 1 fs time step,



constant pressure (1 atm) and periodic boundary conditions. Long-range electrostatic interactions were simulated using PME (Particle Mesh Ewald) method [57]. Non-bonding interactions were updated every 25 steps and data were collected every 1 ps. All plots were created and fitted using GNUPLOT [58], Origin [59] and MS EXCEL program. Spatial Distribution Analysis was performed by using Travis [60] and VMD program [61].

Results and discussion

In the case of ionic liquid the description of the electrostatic interactions is the key to reproduce experimental results by using MD simulations with empirical force field. However, the scaling factor which mimics polarizability has to be used with extreme caution, due to the fact, that the details in the radial distribution function (RDF) are lost, as the charges on the ions decrease [21,62]. This task seems to be difficult, because the linear change of the charge distribution is causing exponential changes in the mobility as described by the mean-squared displacement (MSD) curves. In the investigated range of the charge scaling factor (0.88 to 1.0) we did not observe any significant change in the shape of the RDFs as shown in Fig 2. With the temperature increase the value of the first maximum responsible for the description of the most probable cation-anion distance, was decreased and the peak was flattened. We observed this tendency with the charge scaling factor of 0.92 and 0.88, after crossing the IL melting temperature. This effect was caused by an increased mobility of the ions for temperatures higher than melting temperature. With the scaling factor of 0.96 and 1.00, before and after crossing the experimentally measured melting point temperature, the RDF plots are almost identical. This effect is visible in the case of all analyzed interactions (cation-anion, anion-anion and cation-cation). To analyze in detail the cation-anion relationships, we performed Spatial Distribution Function (SDF) analysis as shown on Fig. 3. In the case of both analyzed ionic liquids the most probable cation-anion interaction place is located with the hydrogen atom in the vicinity of the nitrogen from the pyridine ring. This is due to the highest difference in the partial charge. Due to the presence of the highly mobile alkyl chain, the interaction area is rotated against the pyridine ring. There is the second interaction area with the second hydrogen atom from the pyridine ring. In this case we also observed the rotation, however it is caused by the cation-cation interaction. Additionally, we observed a π - π interaction type as available on both sides of the pyridine ring. After crossing the melting temperature, the first area of the cation-cation interactions is gone, due to the increased mobility of the anions. All blue spots visible on Fig. 3 corresponds to the second interaction area around 15 Å as visible on the RDF plots.

To observe in detail the change of the mobility of the ions as a function of the temperature for different charge scaling factors, we have calculated mean square displacement (MSD) curves. The MSD allows for easy calculation of self-diffusion coefficient. The first step to do so, is the linear regression of the MSD plots, to obtain time related MSD. In our case it is nano second time scale [$\text{\AA}^2/\text{ns}$], and in the manuscript will be called MSD-ns. This value can be placed directly to the Einstein formula for calculation of the self-diffusion coefficient D_i .

$$D_i = \lim_{t \rightarrow \infty} \frac{d}{dt} \frac{1}{6} \langle [r_i(t) - r_i(0)]^2 \rangle$$

Other physicochemical parameters such as viscosity, ionic conductivity or thermal conductivity depend mostly on diffusion. Therefore the calculation of the mobility is the key for a proper theoretical prediction of the physical properties of ILs. The direct correlation between diffusion and viscosity is defined by the Stokes-Einstein equation, in which those values are inverse proportional [63,64,65].

MSD plots calculated from MD simulations of [b4mpy][BF₄] with different box sizes are presented on Fig. 4. For the small system with only 216 ion pairs, the deviation from the linear lines are quite large and can be associated with local ordering and faster/slower movement of some ions. For larger systems with 512 or 1000 ions pairs MSD plots do not deviate from linear lines. With the large enough molecular system, the local deviations are not statistically important and does not have a big influence for the obtained MSD-ns. The summary of the obtained MSD-ns values are shown on Fig. 5. Our result show, that for MD simulation with 1.0 and 0.96 scaling factor, MSD-ns values are very small for all temperatures. The results with scaling factor 0.88 are in the best agreement with experimental data, since the MSD plots (see Fig. 5) fits best to the viscosity plot [27]. However, in this case, the estimation error is up to 50%. With the charge scaling factor of 0.7, the estimation error can be even up to 80% as shown by Sprenger et al. [56].

The most adequate way for calculation of the melting temperature for ionic liquids seems to be the Pseudo-Supercritical Path (PSCP) method postulated by Margin and co-workers [20,66], however, its application is rather problematic. According to the Lindemann criterion, the melting occurs, when the thermal motion of the atoms of the crystal reaches MSD of about one tenth of the interatomic distance [67,68]. It can be briefly defined as $(\text{MSD}/d^2) \sim 0.1$, where “d” is the average intermolecular distance. In the case of the liquids, such universal criterion does not exist, but have to be found individually, as it was shown by Niss et al. [69]. The authors named it as the *intrinistic* Lindemann coefficient. In the crystals MSD comes mostly from the vibrations, in the case of the liquids, the major contribution comes from

displacements. With the temperature increase in the crystals, the ordered state melts at T_m , whereas in the amorphous state the disordered structure softens at the glass transition temperature T_g , above which the flow connected with the viscosity, occurs [70]. The empirical law $T_g \approx 2/3 T_m$ suggest that those two phenomena have a common basis [71]. Many ILs slowly form glasses at low temperatures, because they have negligible vapor pressures. In general, they do not evaporate or boil at high temperatures [72]. In our case the melting temperatures for ([b4mpy][BF₄]) and ([b4mpy][Cl]) are about 303 and 333 K, respectively. It suggest the following glass transition temperatures: 202 and 222 K for ([b4mpy][BF₄]) and ([b4mpy][Cl]), respectively. This prediction holds well, since the glass transition temperature T_g for ([b4mpy][BF₄]) is 203 K [73]. In such a low temperature it is very difficult to catch a proper MSD value to identify the glass transition temperature. Therefore the direct identification of the melting temperature, seems to be a better solution. The straightforward calculation, from the MD simulation with the temperature restraints of the melting point temperature, can be overestimated or underestimated, due to the existence of the superheating / supercooling phenomenon [20,74]. To avoid that problem we decided to perform a set of 10 ns long MD simulations in a wide range of temperatures. As a consequence the estimation error was within temperature step. In the case of ([b4mpy][BF₄]) the experimentally measured melting temperature is 303 K [45]. The mean square displacements (MSD-ns) in 300K were 3.06 and 2.34 and in 310 K were 5.07 and 3.30 [$\text{\AA}^2/\text{ns}$] for cation and anion, respectively (see Fig 5). The average cation – anion distances at 300 and 310 K were 4,7 and 4,8 \AA as identified with the RDF plots (see Fig. 2 and supplementary data). The experimentally measured melting temperature of ([b4mpy][Cl]), is about 333K. According to our calculation the average distance between cation and anion is about 4.5 \AA in 340 and 350K. The mean square displacements (MSD-ns) are 2.44 and 2.36 in 340 K and 8.24 and 6.40 in 350 K for cation and anion, respectively (see Fig 5). The summary of the calculation of the so called by Niss et al. [69] *intrinsic* Lindemann criterion are summarized in Table 1.

Table 1. The summary of the calculation of the *intrinsic* Lindemann coefficient for both simulated ionic liquids. The units of the diffusion coefficients are [$\text{\AA}^2/\text{ns}$], the average distances are in [\AA].

([b4mpy][BF4])				([b4mpy][Cl])			
300K		310K		340K		350K	
cation	anion	cation	anion	cation	anion	cation	anion
$\frac{3.06}{4.7^2} = 0.138$	$\frac{2.34}{4.7^2} = 0.106$	$\frac{5.07}{4.8^2} = 0.220$	$\frac{3.30}{4.8^2} = 0.143$	$\frac{2.44}{4.5^2} = 0.120$	$\frac{2.36}{4.5^2} = 0.116$	$\frac{8.24}{4.5^2} = 0.407$	$\frac{6.40}{4.5^2} = 0.316$

According to Larini et al. [70] the ratio of MSD/d^2 is close to 0.129 for the melting of a hard-sphere face-centred cubic solid. In the case of ionic liquids, this value seems to be a little bit higher. According to our results, in the melting temperature, the ratio of ($[\text{MSD-ns}] / d^2$) is about 0.20 and 0.14 for cation and anion, respectively. The differences are caused by the fact, that the diffusion coefficient for the anion is smaller, than for the cation [17]. In general we can postulate, that in the MD simulations the melting temperature will be crossed, when the MSD will be greater than the average distance between cation and anion.

The self-diffusion coefficient of ionic liquid is the most important factor in determination of the ionic conductivity. In this work we calculated the ionic conductivity of [b4mpy][BF₄] by using the nerst-Einstein equation, and compared it with available experimental data [73] (see Fig. 6).

$$\sigma_c = \frac{Ne^2(D_{self(cat)} + D_{self(an)})}{Vk_B T}$$

[σ_c – ionic conductivity; N – number of ions in the simulation cell; T – temperature; e – electron charge; k_B – Boltzmann’s constant; D_{self} – self-diffusion coefficient, as obtained with Einstein formula.]

With the charge scaling factor of 0.88, the obtained ionic conductivity is systematically lower, with an error similar as in the prediction of the viscosity (about 50%). Picalek and Kolafa [75] are explaining this phenomenon by a short-time clustering which is caused by the correlation in the ion motion. With the decrease of the charge scaling factor, the interactions in the clusters are weaker and the ion motion is higher.

Density of IL is a static parameter which is less sensitive to the charges used in parameterization of empirical force field used in MD simulation than a dynamic parameter as diffusion coefficient. Densities calculated from MD simulations of [b4mpy][BF₄] at

temperatures from 270 to 390 K are compared to experimental data on Fig. 7. In contrast to MSD, the results from the density calculation, with charge scaling factor 0.88 are further from experimental data than results with scaling factor 1.0. However, both sets of simulations properly describe linear dependency of the density on temperature.

Conclusions

We performed 60 simulations for 1-butyl-4-methylpyridinium tetrafluoroborate ([b4mpy][BF₄]) and for 1-butyl-4-methylpyridinium chloride ([b4mpy][Cl]) testing different sizes of the simulation system in different temperatures and with different charge scaling factors. The minimal size of the simulated system have to be at least 500 cation-anion pairs. The size of the simulated system affects calculation of mean square displacement and only for large enough molecular system, MSD curves are linear. In the case of the small molecular system, the local disturbances have a large influence on the obtained result. Scaling down all partial charges by a factor of 0.88 is a simple solution to mimic polarization effect in IL and gives adequate description of ionic mobility and its changes with temperature. The charge scaling factor of 1.00 and 0.96 does not reproduce the diffusion coefficient and as a consequence viscosity and the other diffusion based properties. Molecular dynamics simulation is able to predict viscosity and ionic conductivity, however, our results show, that the error is highly dependent on the charge scaling factor. While the charge scaling factor decreases, the estimation error of the viscosity and ionic conductivity decreases as well. In our case the estimation error was up to 50%. MD is a good tool for the structural description, however we are losing some structural information with the decrease of the charge scaling factor. According to our results, the best compromise is 0.88. Using *intrinsic* Lindemann criterion of about 0.20 and 0.14 for cation and anion, respectively, we are able to identify the investigated IL melting point with an error less than 5%. However, to extend this statement for the other IL's, further investigation is needed. We were able to predict density and radial distribution functions which are less sensitive to the charge parameterization used in the simulations. In the case of the density, MD simulation was able to reproduce properly linear dependency on temperature with the estimation error less than 5%.



Acknowledgements

This work was supported by Switzerland through the Swiss Contribution to the enlarged European Union [grant number PSPB-051/2010]. Calculations were carried out at the supercomputers of Informatics Center of the Metropolitan Academic Network (IC MAN) at the Gdansk University of Technology in Poland

ACCEPTED MANUSCRIPT

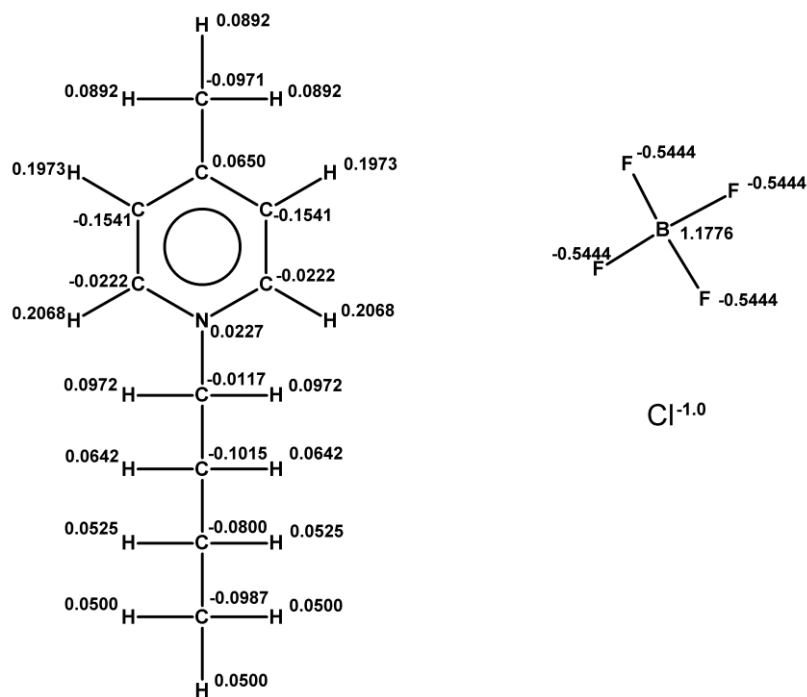


Fig. 1. Partial charges calculated for ([b4mpy][BF₄]) and ([b4mpy][Cl]) ions using antechamber AM1-BCC method.

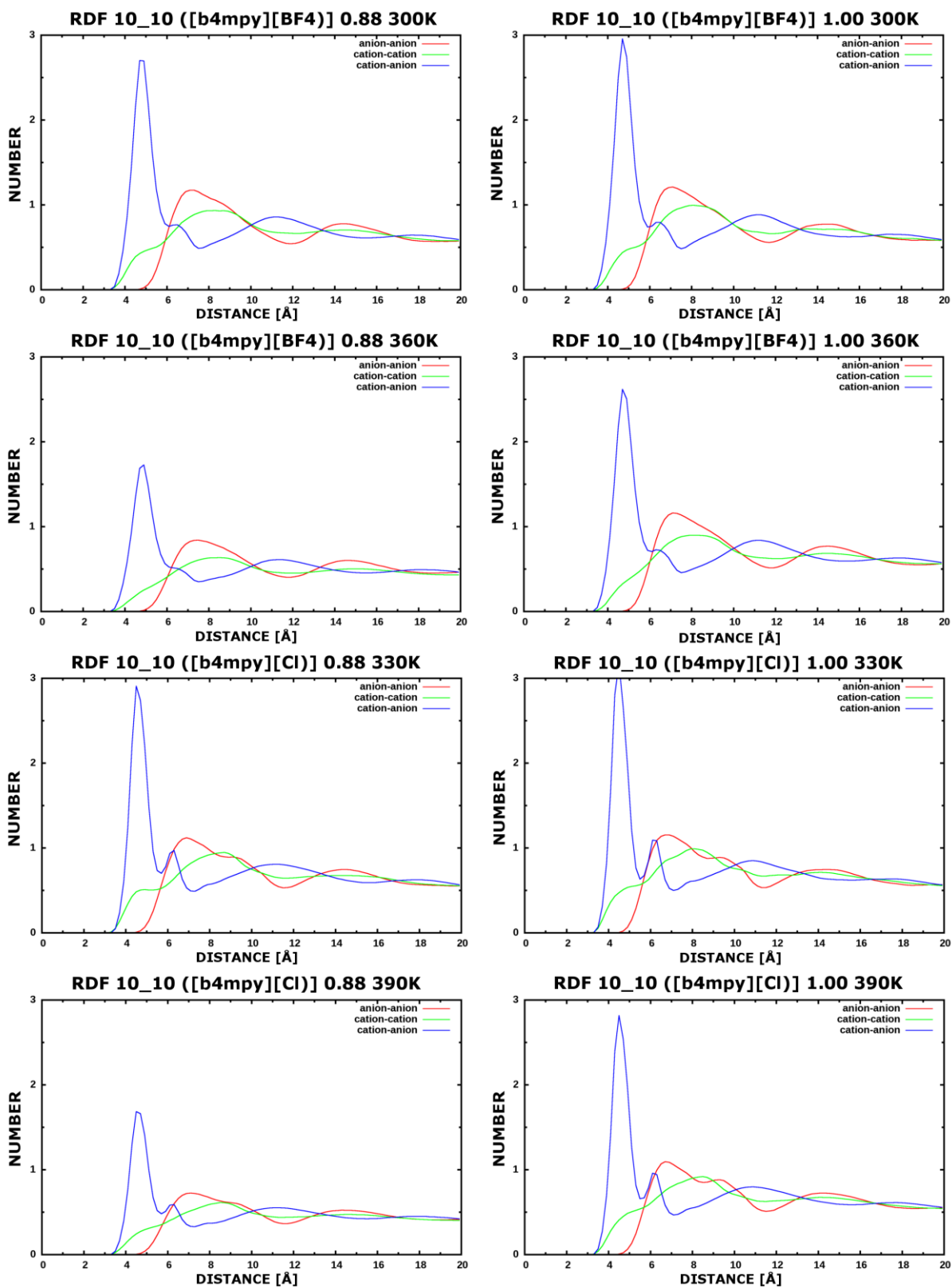


Fig 2. Radial distribution function (RDF) for $([b4mpy][BF_4])$ and $([b4mpy][Cl])$ ionic liquid calculated from MD simulations with 0.88 and 1.0 charge scaling factors, before and after crossing melting temperature. All plots correspond to the system size of $10 \times 10 \times 10$ (10_{10}) cation-anion pairs.

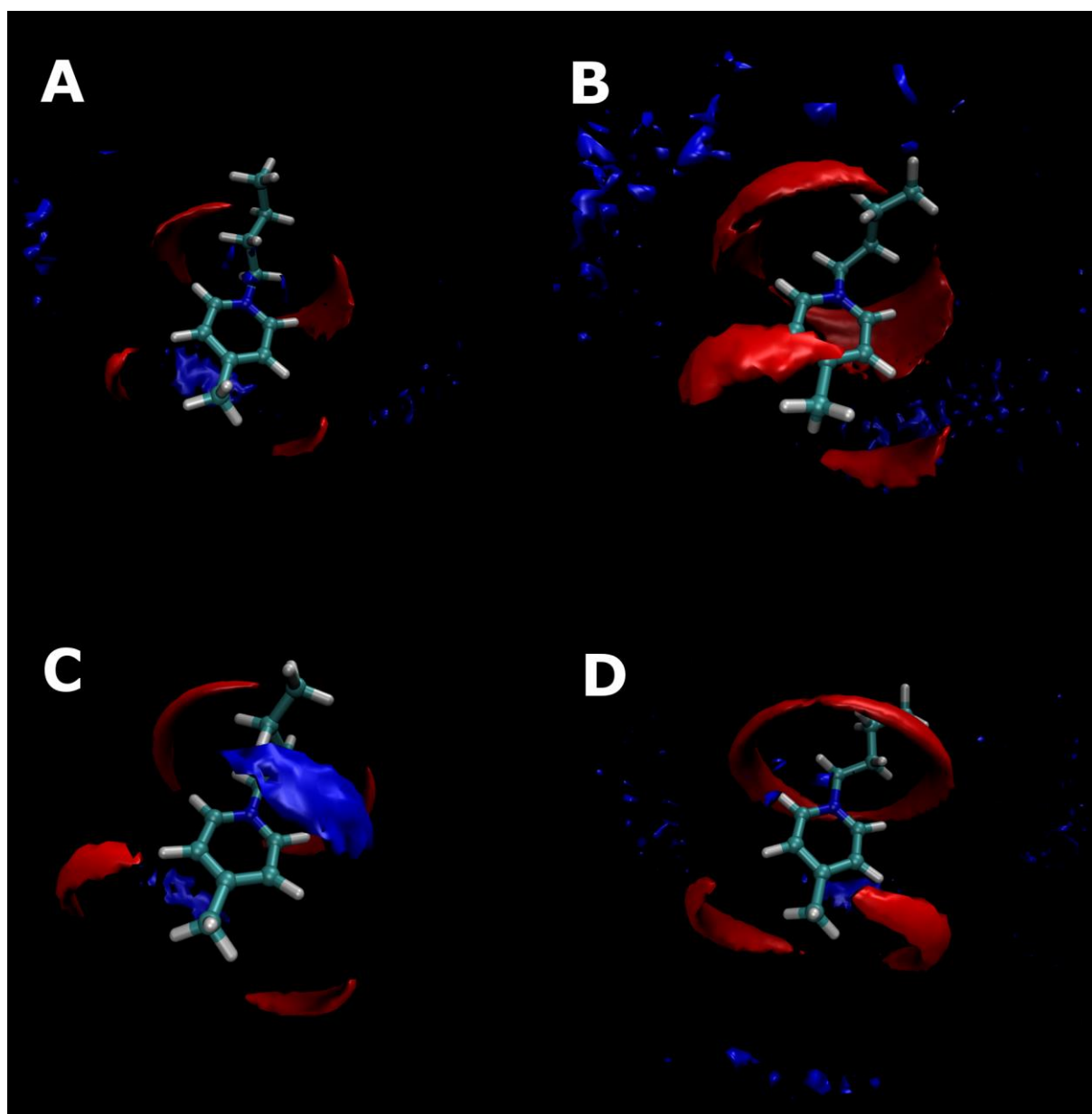


Fig 3. Spatial distribution function (SDF) for ([b4mpy][BF₄]) (top, A – 300K and B – 360K) and ([b4mpy][Cl]) (bottom, C – 330K and D – 390K). The red area corresponds to the location of the anion around the cation, the blue area corresponds to the location of the cation. All plots are taken in the distance of 0.4 Å in the case of the anion and 1.4 Å in the case of the cation from the first maximum of interactions as visible on RDF plots. Fig. A corresponds to 51 and 55 % of population in the case of the cation and anion, respectively. Fig. B – 50 and 49 %, Fig. C and D – 48 and 55 % of population. One have to take the account, that after crossing the melting temperature, the first sphere of the cation-cation interactions is gone and the blue spots belong to the second peak on the RDF plots. Both ionic liquids are with the 0.88 charge scaling factor.

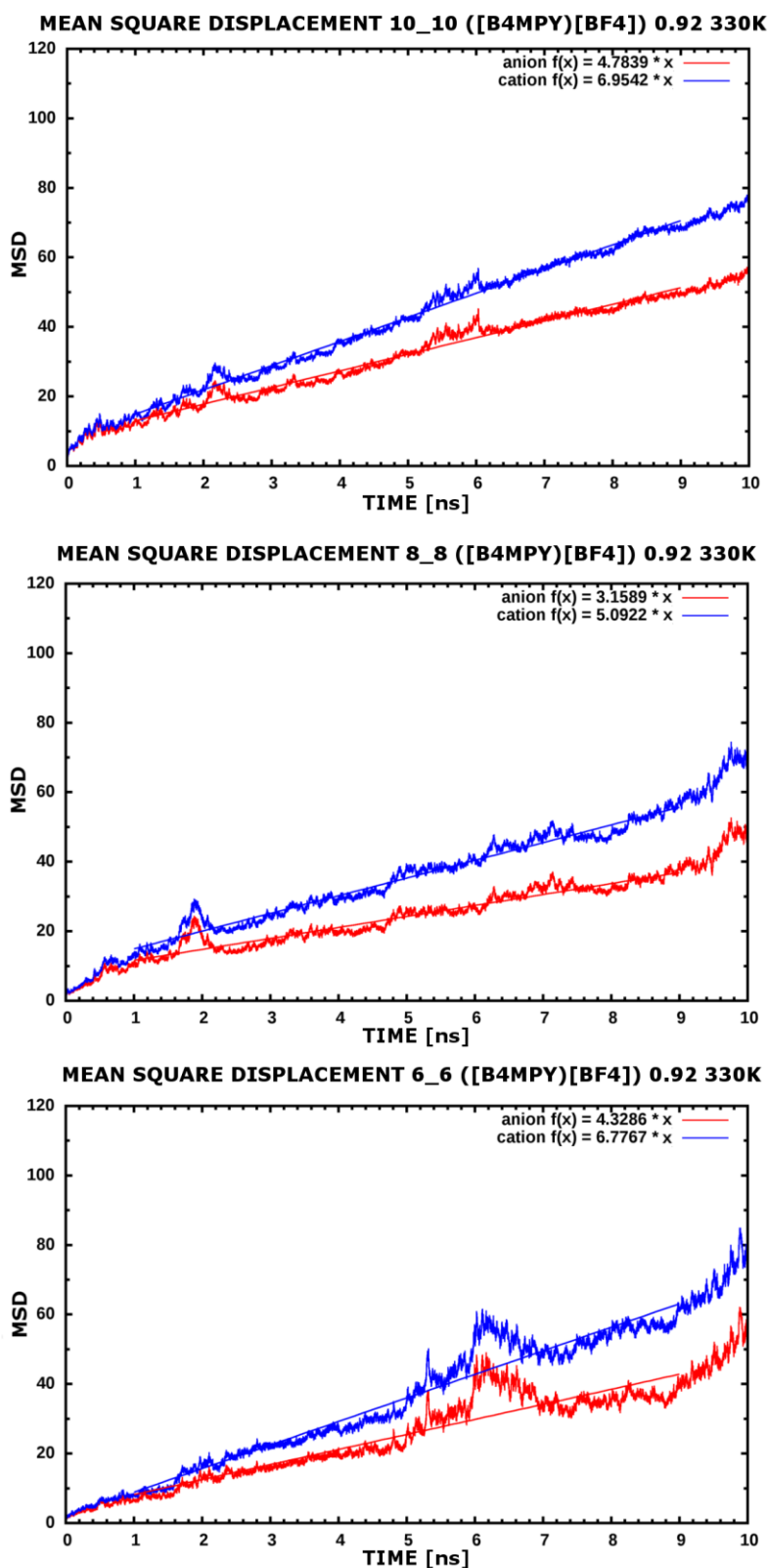


Fig 4. Mean square displacement (MSD) [\AA^2] plots for [b4mpy][BF₄] with different box size: 1000 (10_10) ion pairs (top), 512 (8_8) ion pairs (middle), 216 (6_6) ion pairs (bottom). The linear approximation are given on the top right on the plots. The slope coefficient is called in the manuscript, diffusion coefficient [$\text{\AA}^2/\text{ns}$].

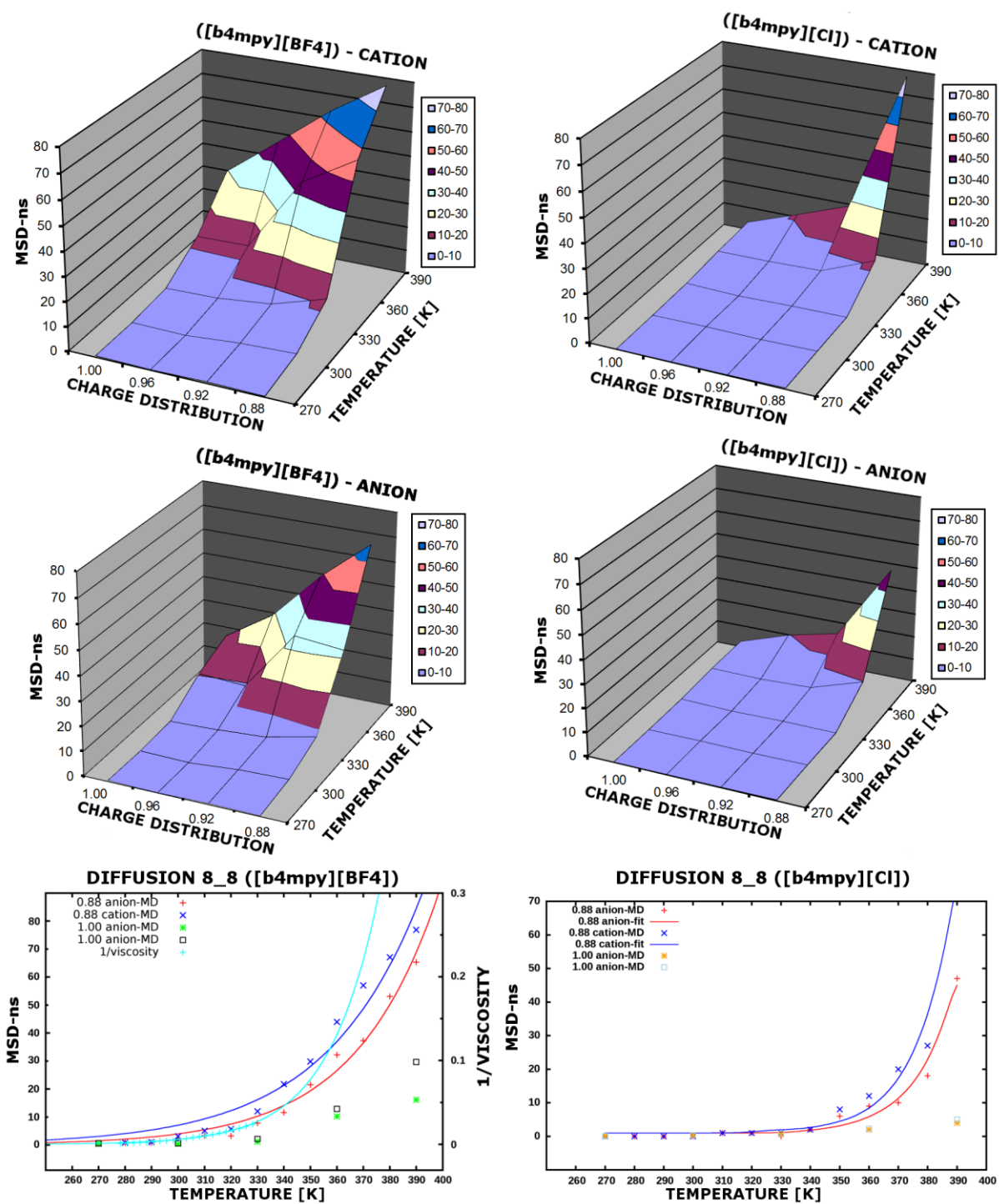


Fig 5. Mean square displacement as a function of temperature and charge scaling factor used in the simulations. Viscosity data, as shown on the bottom-left plot (light-blue) are taken from Bandres et al [27].

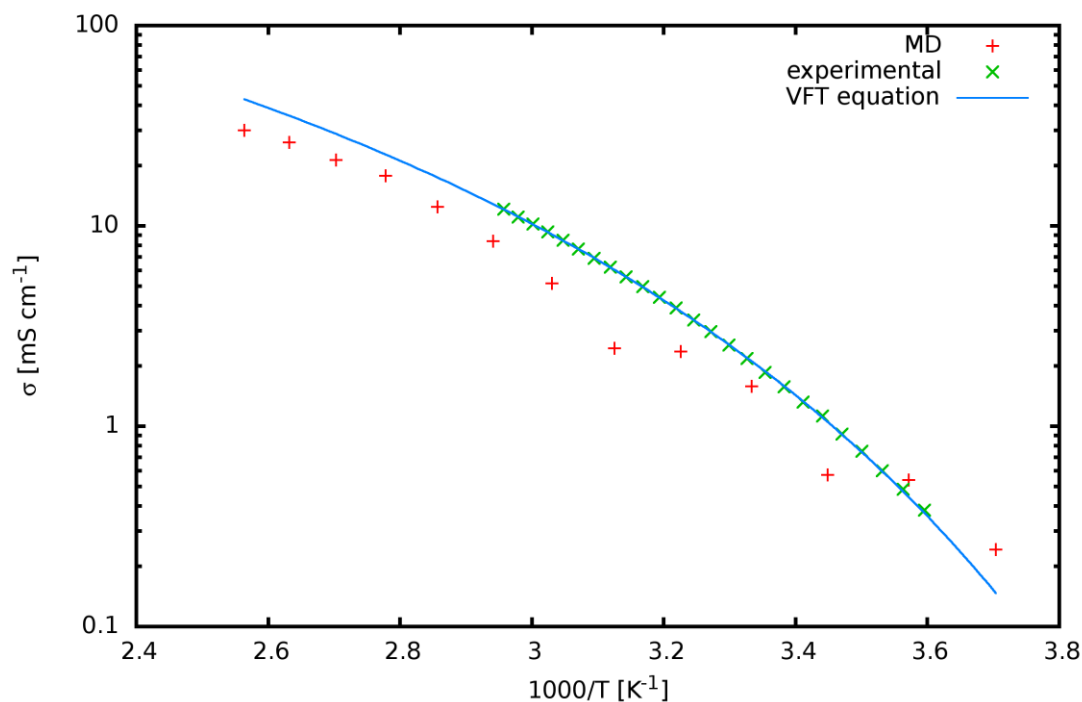


Fig 6. The electrical conductivity, σ , in a function on the inverse of the absolute temperature for $([\text{b4mpy}][\text{BF}_4])$. VTF – Vogel-Fulcher-Tammann equation. Experimental data are taken from Bandres et al. [73].

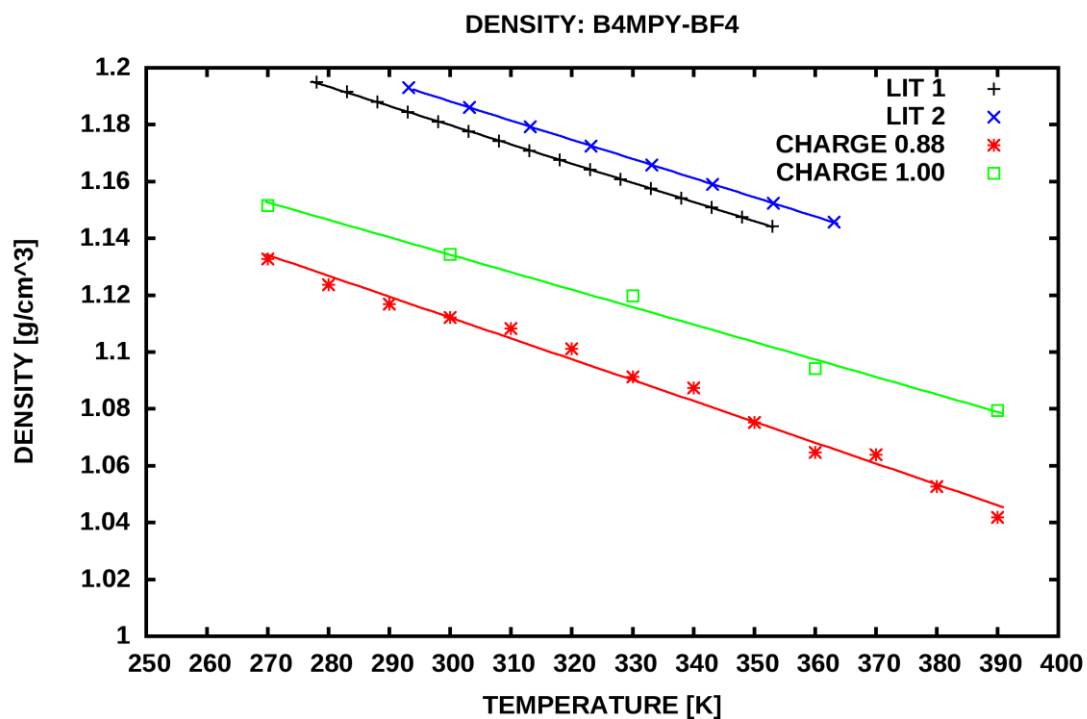
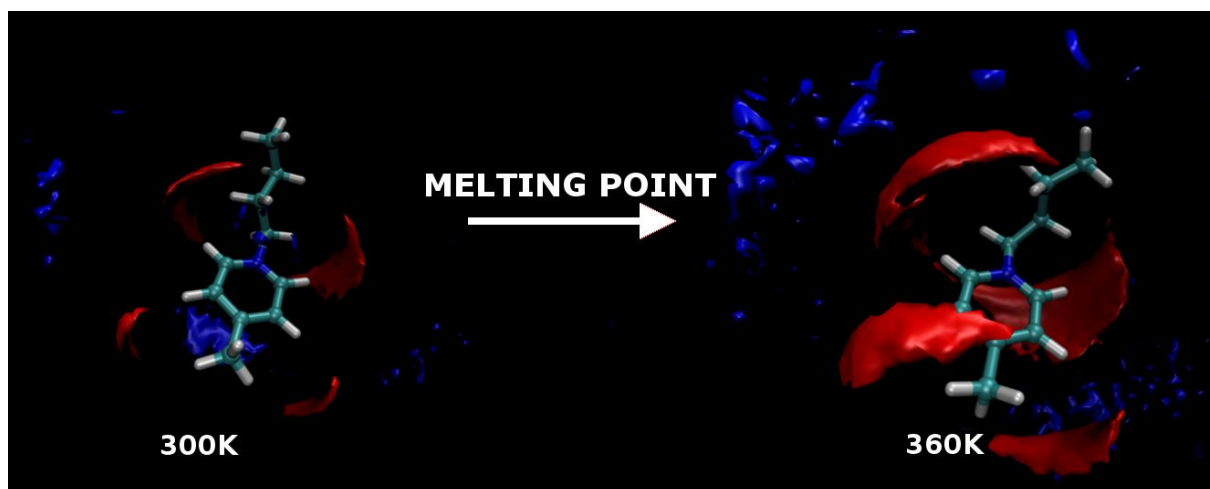


Fig 7. Density calculated from MD simulations of $([\text{b4mpy}][\text{BF}_4])$ as a function of the absolute temperature, compared to experimental data (LIT 1: Nonthanasin et al. [33], LIT 2: Sanchez et al. [28].)

References:



Graphical abstract

ACCEPTED MANUSCRIPT

Highlights

Molecular dynamics simulation is able to predict density, viscosity and ionic conductivity of ILs.

Scaling down partial charges can mimic polarization and is necessary to reproduce physico-chemical properties of ILs in MD.

Intrinsic Lindemann criterion can identify the ILs melting point, the increased mobility is shown on SDF plots.

Insufficient size of the simulated system can effect in large local disturbances.

1. M. Palacio, B. Bhushan, A Review of Ionic Liquids for Green Molecular Lubrication in Nanotechnology, *Tribology Letters*. 40 (2010) 247–268. doi:10.1007/s11249-010-9671-8.
2. S. Keskin, D. Kayrak-Talay, U. Akman, Ö. Hortaçsu, A review of ionic liquids towards supercritical fluid applications, *The Journal of Supercritical Fluids*. 43 (2007) 150–180. doi:10.1016/j.supflu.2007.05.013.
3. M. Freemantle, DESIGNER SOLVENTS: Ionic liquids may boost clean technology development, *Chemical & Engineering News*. 76 (1998) 32–37. doi:10.1021/cen-v076n013.p032.
4. C. Chiappe, D. Pieraccini, Ionic liquids: solvent properties and organic reactivity, *Journal of Physical Organic Chemistry*. 18 (2005) 275–297. doi:10.1002/poc.863.
5. A.R. Katritzky, R. Jain, A. Lomaka, R. Petrukhin, M. Karelson, A.E. Visser, R.D. Rogers, Correlation of the Melting Points of Potential Ionic Liquids (Imidazolium Bromides and Benzimidazolium Bromides) Using the CODESSA Program, *Journal of Chemical Information and Computer Sciences*. 42 (2002) 225–231. doi:10.1021/ci0100494.
6. D.M. Eike, J.F. Brennecke, E.J. Maginn, Predicting melting points of quaternary ammonium ionic liquids Electronic supplementary information (ESI) available: training sets B and C. See <http://www.rsc.org/suppdata/gc/b3/b301217d/>, *Green Chemistry*. 5 (2003) 323. doi:10.1039/b301217d.
7. R. Bini, M. Malvaldi, W.R. Pitner, C. Chiappe, QSPR correlation for conductivities and viscosities of low-temperature melting ionic liquids, *Journal of Physical Organic Chemistry*. 21 (2008) 622–629. doi:10.1002/poc.1337.
8. H. Matsuda, H. Yamamoto, K. Kurihara, K. Tochigi, Computer-aided reverse design for ionic liquids by QSPR using descriptors of group contribution type for ionic conductivities and viscosities, *Fluid Phase Equilibria*. 261 (2007) 434–443. doi:10.1016/j.fluid.2007.07.018.
9. I. Billard, G. Marcou, A. Ouadi, A. Varnek, In Silico Design of New Ionic Liquids Based on Quantitative Structure–Property Relationship Models of Ionic Liquid Viscosity, *The Journal of Physical Chemistry B*. 115 (2011) 93–98. doi:10.1021/jp107868w.
10. J. Forsman, C.E. Woodward, M. Trulsson, A Classical Density Functional Theory of Ionic Liquids, *The Journal of Physical Chemistry B*. 115 (2011) 4606–4612. doi:10.1021/jp111747w.
11. C.-W. Cho, U. Preiss, C. Jungnickel, S. Stolte, J. Arning, J. Ranke, A. Klamt, I. Krossing, J. Thöming, Ionic Liquids: Predictions of Physicochemical Properties with Experimental

- and/or DFT-Calculated LFER Parameters To Understand Molecular Interactions in Solution, *The Journal of Physical Chemistry B*. 115 (2011) 6040–6050. doi:10.1021/jp200042f.
12. J.M. Slattery, C. Daguene, P.J. Dyson, T.J.S. Schubert, I. Krossing, How to Predict the Physical Properties of Ionic Liquids: A Volume-Based Approach, *Angewandte Chemie International Edition*. 46 (2007) 5384–5388. doi:10.1002/anie.200700941.
13. D. Wileńska, I. Anusiewicz, S. Freza, M. Bobrowski, E. Laux, S. Uhl, H. Keppner, P. Skurski, Predicting the viscosity and electrical conductivity of ionic liquids on the basis of theoretically calculated ionic volumes, *Molecular Physics*. 113 (2015) 630–639. doi:10.1080/00268976.2014.964344.
14. E. Hawlicka, T. Długoborski, Molecular dynamics simulations of the aqueous solution of tetramethylammonium chloride, *Chemical Physics Letters*. 268 (1997) 325–330. doi:10.1016/S0009-2614(97)00229-7.
15. E.J. Maginn, Molecular simulation of ionic liquids: current status and future opportunities, *Journal of Physics: Condensed Matter*. 21 (2009) 373101. doi:10.1088/0953-8984/21/37/373101.
16. S.U. Lee, J. Jung, Y.-K. Han, Molecular dynamics study of the ionic conductivity of 1-n-butyl-3-methylimidazolium salts as ionic liquids, *Chemical Physics Letters*. 406 (2005) 332–340. doi:10.1016/j.cplett.2005.02.109.
17. C.E. Resende Prado, L.C. Gomide Freitas, Molecular dynamics simulation of the room-temperature ionic liquid 1-butyl-3-methylimidazolium tetrafluoroborate, *Journal of Molecular Structure: THEOCHEM*. 847 (2007) 93–100. doi:10.1016/j.theochem.2007.09.009.
18. T. Köddermann, D. Paschek, R. Ludwig, Molecular Dynamic Simulations of Ionic Liquids: A Reliable Description of Structure, Thermodynamics and Dynamics, *ChemPhysChem*. 8 (2007) 2464–2470. doi:10.1002/cphc.200700552.
19. J. Picálek, B. Minofar, J. Kolafa, P. Jungwirth, Aqueous solutions of ionic liquids: study of the solution/vapor interface using molecular dynamics simulations, *Physical Chemistry Chemical Physics*. 10 (2008) 5765. doi:10.1039/b806205f.
20. Y. Zhang, E.J. Maginn, A comparison of methods for melting point calculation using molecular dynamics simulations, *The Journal of Chemical Physics*. 136 (2012) 144116. doi:10.1063/1.3702587.
21. T.G.A. Youngs, C. Hardacre, Application of Static Charge Transfer within an Ionic-Liquid Force Field and Its Effect on Structure and Dynamics, *ChemPhysChem*. 9 (2008) 1548–1558. doi:10.1002/cphc.200800200.
22. M.H. Kowsari, S. Alavi, M. Ashrafizaadeh, B. Najafi, Molecular dynamics simulation of imidazolium-based ionic liquids. I. Dynamics and diffusion coefficient, *The Journal of Chemical Physics*. 129 (2008) 224508. doi:10.1063/1.3035978.
23. M.H. Kowsari, S. Alavi, M. Ashrafizaadeh, B. Najafi, Molecular dynamics simulation of imidazolium-based ionic liquids. II. Transport coefficients, *The Journal of Chemical Physics*. 130 (2009) 014703. doi:10.1063/1.3042279.
24. S.A. Kislenco, I.S. Samoylov, R.H. Amirov, Molecular dynamics simulation of the electrochemical interface between a graphite surface and the ionic liquid [BMIM][PF₆], *Physical Chemistry Chemical Physics*. 11 (2009) 5584. doi:10.1039/b823189c.
25. M. Klähn, G.S. Lim, P. Wu, How ion properties determine the stability of a lipase enzyme in ionic liquids: A molecular dynamics study, *Physical Chemistry Chemical Physics*. 13 (2011) 18647. doi:10.1039/c1cp22056j.
26. A. Heintz, J.K. Lehmann, C. Wertz, Thermodynamic Properties of Mixtures Containing Ionic Liquids. 3. Liquid–Liquid Equilibria of Binary Mixtures of 1-Ethyl-3-methylimidazolium Bis(trifluoromethylsulfonyl)imide with Propan-1-ol, Butan-1-ol, and

- Pentan-1-ol[†], *Journal of Chemical & Engineering Data*. 48 (2003) 472–474.
doi:10.1021/je0201931.
27. I. Bandrés, B. Giner, H. Artigas, F.M. Royo, C. Lafuente, Thermophysical Comparative Study of Two Isomeric Pyridinium-Based Ionic Liquids, *The Journal of Physical Chemistry B*. 112 (2008) 3077–3084. doi:10.1021/jp077259p.
28. L.G. Sánchez, J.R. Espel, F. Onink, G.W. Meindersma, A.B. de Haan, Density, Viscosity, and Surface Tension of Synthesis Grade Imidazolium, Pyridinium, and Pyrrolidinium Based Room Temperature Ionic Liquids, *Journal of Chemical & Engineering Data*. 54 (2009) 2803–2812. doi:10.1021/je800710p.
29. J. Safarov, I. Kul, W.A. El-Awady, J. Nocke, A. Shahverdiyev, E. Hassel, Thermophysical properties of 1-butyl-4-methylpyridinium tetrafluoroborate, *The Journal of Chemical Thermodynamics*. 51 (2012) 82–87. doi:10.1016/j.jct.2012.02.018.
30. M. García-Mardones, A. Barrós, I. Bandrés, H. Artigas, C. Lafuente, Thermodynamic properties of binary mixtures combining two pyridinium-based ionic liquids and two alkanols, *The Journal of Chemical Thermodynamics*. 51 (2012) 17–24. doi:10.1016/j.jct.2012.02.023.
31. H. Guerrero, M. García-Mardones, P. Cea, C. Lafuente, I. Bandrés, Correlation of the volumetric behaviour of pyridinium-based ionic liquids with two different equations, *Thermochimica Acta*. 531 (2012) 21–27. doi:10.1016/j.tca.2011.12.020.
32. M. García-Mardones, I. Gascón, M.C. López, F.M. Royo, C. Lafuente, Viscosimetric Study of Binary Mixtures Containing Pyridinium-Based Ionic Liquids and Alkanols, *Journal of Chemical & Engineering Data*. 57 (2012) 3549–3556. doi:10.1021/je300557g.
33. T. Nonthanasin, A. Henni, C. Saiwan, Densities and low pressure solubilities of carbon dioxide in five promising ionic liquids, *RSC Advances*. 4 (2014) 7566. doi:10.1039/c3ra46339g.
34. J. Ortega, R. Vreekamp, E. Penco, E. Marrero, Mixing thermodynamic properties of 1-butyl-4-methylpyridinium tetrafluoroborate [b4mpy][BF₄] with water and with an alkan-1-ol (methanol to pentanol), *The Journal of Chemical Thermodynamics*. 40 (2008) 1087–1094. doi:10.1016/j.jct.2008.02.019.
35. M.B. Shiflett, B.A. Elliott, A. Yokozeki, Phase behavior of vinyl fluoride in room-temperature ionic liquids [emim][Tf₂N], [bmim][N(CN)₂], [bmpy][BF₄], [bmim][HFPS] and [omim][TFES], *Fluid Phase Equilibria*. 316 (2012) 147–155. doi:10.1016/j.fluid.2011.11.030.
36. M. García-Mardones, H.M. Osorio, C. Lafuente, I. Gascón, Ionic Conductivities of Binary Mixtures Containing Pyridinium-Based Ionic Liquids and Alkanols, *Journal of Chemical & Engineering Data*. 58 (2013) 1613–1620. doi:10.1021/je301347v.
37. Y. Li, M. Zhang, Q. Liu, H. Su, Phase behaviour for aqueous two-phase systems containing the ionic liquid 1-butylpyridinium tetrafluoroborate/1-butyl-4-methylpyridinium tetrafluoroborate and organic salts (sodium tartrate/ammonium citrate/trisodium citrate) at different temperatures, *The Journal of Chemical Thermodynamics*. 66 (2013) 80–87. doi:10.1016/j.jct.2013.06.011.
38. S.I. Abu-Eishah, A.M. Dowaidar, Liquid–Liquid Equilibrium of Ternary Systems of Cyclohexane + (Benzene, + Toluene, + Ethylbenzene, or + *o*-Xylene) + 4-Methyl- *N*-butyl Pyridinium Tetrafluoroborate Ionic Liquid at 303.15 K, *Journal of Chemical & Engineering Data*. 53 (2008) 1708–1712. doi:10.1021/je7007268.
39. S.H. Schöfer, N. Kaftzik, U. Kragl, P. Wasserscheid, Enzyme catalysis in ionic liquids: lipase catalysed kinetic resolution of 1-phenylethanol with improved enantioselectivity, *Chemical Communications*. (2001) 425–426. doi:10.1039/b009389k.
40. G. Inoue, Y. Iwai, M. Yasutake, K. Honda, Y. Arai, Measurement of infinite dilution activity coefficients of *n*-alkanes in 4-methyl-*n*-butylpyridinium tetrafluoroborate using gas–

liquid chromatography, *Fluid Phase Equilibria*. 251 (2007) 17–23.

doi:10.1016/j.fluid.2006.10.016.

41. K.H.A.E. Alkhalidi, M.S. Al-Tuwaim, M.S. Fandary, A.S. Al-Jimaz, Separation of propylbenzene and n-alkanes from their mixtures using 4-methyl-N-butylpyridinium tetrafluoroborate as an ionic solvent at several temperatures, *Fluid Phase Equilibria*. 309 (2011) 102–107. doi:10.1016/j.fluid.2011.06.036.

42. M. Scendo, J. Uznanska, Inhibition Effect of 1-Butyl-4-Methylpyridinium Tetrafluoroborate on the Corrosion of Copper in Phosphate Solutions, *International Journal of Corrosion*. 2011 (2011) 1–12. doi:10.1155/2011/761418.

43. A. Latała, M. Nędzi, P. Stepnowski, Toxicity of imidazolium and pyridinium based ionic liquids towards algae. *Chlorella vulgaris*, *Oocystis submarina* (green algae) and *Cyclotella meneghiniana*, *Skeletonema marinoi* (diatoms), *Green Chemistry*. 11 (2009) 580.

doi:10.1039/b821140j.

44. N. Papaiconomou, J. Estager, Y. Traore, P. Bauduin, C. Bas, S. Legeai, S. Viboud, M. Draye, Synthesis, Physicochemical Properties, and Toxicity Data of New Hydrophobic Ionic Liquids Containing Dimethylpyridinium and Trimethylpyridinium Cations[†], *Journal of Chemical & Engineering Data*. 55 (2010) 1971–1979. doi:10.1021/je9009283.

45. K. Sakizadeh, L.P. Olson, P.J. Cowdery-Corvan, T. Ishida, D.R. Whitcomb, Thermographic materials containing ionic liquids. (2007) US Patent No.: US 7,163,786 B1.

46. I. Bandrés, G. Pera, S. Martín, M. Castro, C. Lafuente, Thermophysical Study of 1-Butyl-2-Methylpyridinium Tetrafluoroborate Ionic Liquid, *The Journal of Physical Chemistry B*. 113 (2009) 11936–11942. doi:10.1021/jp906133t.

47. A. Navas, J. Ortega, J. Palomar, C. Díaz, R. Vreekamp, COSMO-RS analysis on mixing properties obtained for the systems 1-butyl-X-methylpyridinium tetrafluoroborate [X = 2,3,4] and 1, ω -dibromoalkanes [ω = 1–6], *Physical Chemistry Chemical Physics*. 13 (2011) 7751. doi:10.1039/c0cp02169e.

48. S. Ardizzone, C.L. Bianchi, P. Drago, D. Mozzanica, P. Quagliotto, P. Savarino, G. Viscardi, Adsorption of 1-alkyl-4-methylpyridinium salts at solid-liquid and water-air interfaces, *Colloids and Surfaces A: Physicochemical and Engineering Aspects*. 113 (1996) 135–144. doi:10.1016/0927-7757(96)03632-1.

49. T. Heinze, K. Schwikal, S. Barthel, Ionic Liquids as Reaction Medium in Cellulose Functionalization, *Macromolecular Bioscience*. 5 (2005) 520–525.

doi:10.1002/mabi.200500039.

50. A.B. Pereira, A. Rodriguez, M. Blesic, K. Shimizu, J.N. Canongia Lopes, L.P.N. Rebelo, Mixtures of Pyridine and Nicotine with Pyridinium-Based Ionic Liquids, *Journal of Chemical & Engineering Data*. 56 (2011) 4356–4363. doi:10.1021/je2001446.

51. E.S. Sashina, D.A. Kashirskii, G. Janowska, M. Zaborski, Thermal properties of 1-alkyl-3-methylpyridinium halide-based ionic liquids, *Thermochimica Acta*. 568 (2013) 185–188. doi:10.1016/j.tca.2013.06.022.

52. B. Ellis, W. Keim, P. Wasserscheid, Linear dimerisation of but-1-ene in biphasic mode using buffered chloroaluminate ionic liquid solvents, *Chemical Communications*. (1999) 337–338. doi:10.1039/a808346k.

53. D.A. Pearlman, D.A. Case, J.W. Caldwell, W.S. Ross, T.E. Cheatham, S. DeBolt, D. Ferguson, G. Seibel, P. Kollman, AMBER, a package of computer programs for applying molecular mechanics, normal mode analysis, molecular dynamics and free energy calculations to simulate the structural and energetic properties of molecules, *Computer Physics Communications*. 91 (1995) 1–41. doi:10.1016/0010-4655(95)00041-D.

54. D.A. Case, T.E. Cheatham, T. Darden, H. Gohlke, R. Luo, K.M. Merz, A. Onufriev, C. Simmerling, B. Wang, R.J. Woods, The Amber biomolecular simulation programs, *Journal of Computational Chemistry*. 26 (2005) 1668–1688. doi:10.1002/jcc.20290.
55. X. Wu, Z. Liu, S. Huang, W. Wang, Molecular dynamics simulation of room-temperature ionic liquid mixture of [bmim][BF₄] and acetonitrile by a refined force field, *Physical Chemistry Chemical Physics*. 7 (2005) 2771. doi:10.1039/b504681p.
56. K.G. Sprenger, V.W. Jaeger, J. Pfandner, The General AMBER Force Field (GAFF) Can Accurately Predict Thermodynamic and Transport Properties of Many Ionic Liquids, *The Journal of Physical Chemistry B*. 119 (2015) 5882–5895. doi:10.1021/acs.jpcc.5b00689.
57. U. Essmann, L. Perera, M.L. Berkowitz, T. Darden, H. Lee, L.G. Pedersen, A smooth particle mesh Ewald method, *The Journal of Chemical Physics*. 103 (1995) 8577. doi:10.1063/1.470117.
58. Williams, T.; Kelley, C. *Gnuplot 4.5: an interactive plotting program*. (2011), URL <http://gnuplot.info>.
59. Origin (OriginLab, Northampton, MA), URL <http://www.originlab.com>
60. M. Brehm, B. Kirchner, TRAVIS - A Free Analyzer and Visualizer for Monte Carlo and Molecular Dynamics Trajectories, *Journal of Chemical Information and Modeling*. 51 (2011) 2007–2023. doi:10.1021/ci200217w.
61. W. Humphrey, A. Dalke, K. Schulten, VMD: Visual molecular dynamics, *Journal of Molecular Graphics*. 14 (1996) 33–38. doi:10.1016/0263-7855(96)00018-5.
62. M.G. Del Pópolo, R.M. Lynden-Bell, J. Kohanoff, Ab Initio Molecular Dynamics Simulation of a Room Temperature Ionic Liquid, *The Journal of Physical Chemistry B*. 109 (2005) 5895–5902. doi:10.1021/jp044414g.
63. A. Einstein, Über die von der molekularkinetischen Theorie der Wärme geforderte Bewegung von in ruhenden Flüssigkeiten suspendierten Teilchen. *Annalen der Physik* 17 (1905), 549–560. doi: 10.1002/andp.19053220806
64. M.-M. Huang, S. Bulut, I. Krossing, H. Weingärtner, Communication: Are hydrodynamic models suited for describing the reorientational dynamics of ions in ionic liquids? A case study of methylimidazolium tetra(hexafluoroisopropoxy)aluminates, *The Journal of Chemical Physics*. 133 (2010) 101101. doi:10.1063/1.3478221.
65. A.W. Taylor, P. Licence, A.P. Abbott, Non-classical diffusion in ionic liquids, *Physical Chemistry Chemical Physics*. 13 (2011) 10147. doi:10.1039/c1cp20373h.
66. D.M. Eike, E.J. Maginn, Atomistic simulation of solid-liquid coexistence for molecular systems: Application to triazole and benzene, *The Journal of Chemical Physics*. 124 (2006) 164503. doi:10.1063/1.2188400.
67. Lindemann, F.A. The calculation of molecular vibration frequencies. *Physik Z.* 11 (1910), 609-612.
68. U. Buchenau, R. Zorn, M.A. Ramos, Probing cooperative liquid dynamics with the mean square displacement, *Physical Review E*. 90 (2014). doi:10.1103/PhysRevE.90.042312.
69. K. Niss, C. Dalle-Ferrier, B. Frick, D. Russo, J. Dyre, C. Alba-Simionesco, Connection between slow and fast dynamics of molecular liquids around the glass transition, *Physical Review E*. 82 (2010). doi:10.1103/PhysRevE.82.021508.
70. L. Larini, A. Ottochian, C. De Michele, D. Leporini, Universal scaling between structural relaxation and vibrational dynamics in glass-forming liquids and polymers, *Nature Physics*. 4 (2008) 42–45. doi:10.1038/nphys788.
71. A. Hunt, A simple connection between the melting temperature and the glass temperature in a kinetic theory of the glass transition, *Journal of Physics: Condensed Matter*. 4 (1992) L429–L431. doi:10.1088/0953-8984/4/32/001.

72. M. Freemantle, *An Introduction to ionic liquids*, RSC Pub, Cambridge, UK, 2010, (4), 31-40. ISBN: 978-1-84755-161-0.
73. I. Bandrés, D.F. Montaña, I. Gascón, P. Cea, C. Lafuente, Study of the conductivity behavior of pyridinium-based ionic liquids, *Electrochimica Acta*. 55 (2010) 2252–2257. doi:10.1016/j.electacta.2009.11.073.
74. P.M. Agrawal, B.M. Rice, D.L. Thompson, Molecular dynamics study of the melting of nitromethane, *The Journal of Chemical Physics*. 119 (2003) 9617. doi:10.1063/1.1612915.
75. J. Picálek, J. Kolafa, Molecular dynamics study of conductivity of ionic liquids: The Kohlrausch law, *Journal of Molecular Liquids*. 134 (2007) 29–33. doi:10.1016/j.molliq.2006.12.015.

ACCEPTED MANUSCRIPT